Approaching the CDF Top Quark Mass Legacy Measurement in the Lepton+Jets channel with the Matrix Element Method

Andrea Malara

Università di Pisa (Supervisor: Costas Vellidis, FNAL)

September 22, 2016

Top Quark

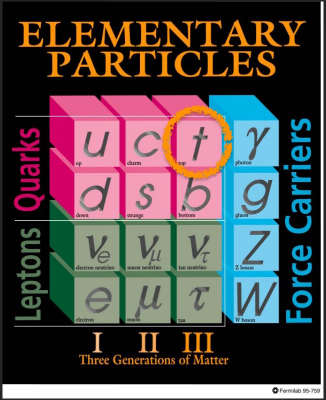

Top Mass

$m_t = 173\ GeV/c^2$

Top Life-Time

$\tau_t = 0.3 \times 10^{-24} s$

Top Quark

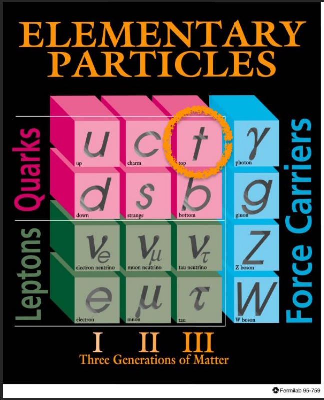

Top Mass

$$m_t = 173\ GeV/c^2$$

Top Life-Time

$$\tau_t = 0.3 \times 10^{-24} s$$

$$\tau_{QCD} = \Lambda_{QCD}^{-1} = 5 \times 10^{-24} s \longrightarrow \text{No hadronization}$$

Top Quark Production

	Quark Annihilation	Gluon Fusion	

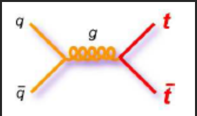

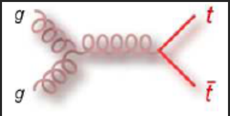

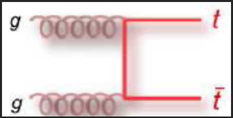

	Quark Annihilation	Gluon Fusion	
Tevatron	85%	15%	$\sigma_t \simeq 7\ pb$
LHC	15%	85%	$\sigma_t \simeq 1\ nb$

Top quark decay mode

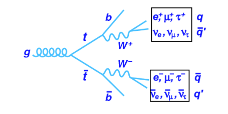

Dilepton events

Low statistic, High S/B

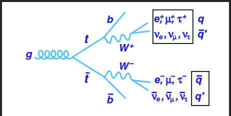

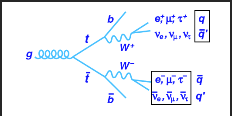

Lepton + jets

Good statistics, Good S/B

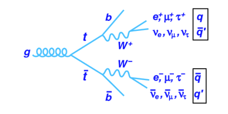

All jets

Good statistics, Low S/B

Top quark decay mode

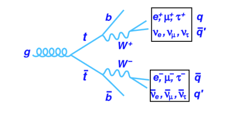

Dilepton events

Low statistic, High S/B

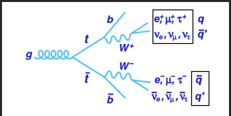

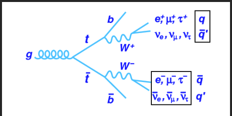

Lepton + jets

Good statistics, Good S/B

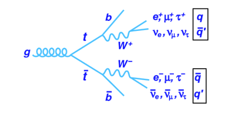

All jets

Good statistics, Low S/B

Why we focus on precise top mass measurement

- Mass is the only top property not predicted by theory.
- Close to electroweak symmetry breaking scale: together with W and H precision physics, provides strong lever for testing the internal consistency of SM .
- The EW vacuum stability depends crucially on the precise top mass value: higher top mass value eventually leads to scenario of metastable or unstable Universe.

Status of measurement

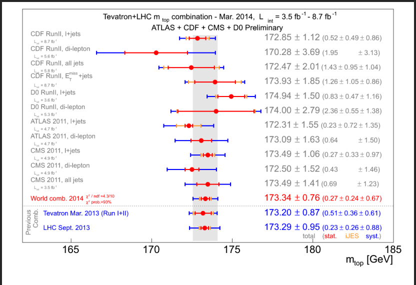

- DØ final measurement in lepton+jets: $m_t = 174.98 \pm 0.76$ GeV$/c^2$.
- CMS measurements in all channels: $m_t = 172.44 \pm 0.48$ GeV$/c^2$.
- Discrepancy of $\sim 3\sigma$.
- We expect that the new CDF top mass measurement will contribute clarifying the discrepancy between the latest DØ and CMS results.
- The goal of the measurement is to reach a total error of less than 0.5%.

Improvements for new CDF data analysis

- More luminosity: from 5.6 fb^{-1} to 9 fb^{-1} $\rightarrow$ 60% more data.
- New event categories: 0-tag, 1-tagL, 2-tagL $\rightarrow$ 30% more events from loose categories.
- Matrix element integration method $\rightarrow$ most precise method.
- Quasi-Monte Carlo technique $\rightarrow$ better accuracy in less time.
- NLO singal MC: POWHEG + PYTHIA $\rightarrow$ reduction of uncertainty.
- Likelihood background included.

Event selection

	0-tag	1-tagL	1-tagT	2-tagL	2-tagT
Lepton E_T	> 20	> 20	> 20	> 20	> 20
Lepton $\lvert\eta\rvert$	< 1.0	< 1.0	< 1.0	< 1.0	< 1.0
$\not{E}_T$	> 20	> 20	> 20	> 20	> 20
3 jets E_T	> 20	> 20	> 20	> 20	> 20
3 jets $\lvert\eta\rvert$	< 2.0	< 2.0	< 2.0	< 2.0	< 2.0
4^{th} jets E_T	> 20	> 12	> 20	> 12	> 20
4^{th} jets $\lvert\eta\rvert$	< 2.0	< 2.4	< 2.0	< 2.4	< 2.0
Extra jets		Any loose or ≥ 1 tight	Any loose	Any loose or ≥ 1 tight	Any loose

Sample composition

	0-tag	1-tagL	1-tagT	2-tagL	2-tagT	All
W+ h.f	697	357	161	34	21	1269
W+ l.f	1581	171	77	3	2	1834
Z+ jets	169	25	14	2	1	212
Diboson	166	31	18	3	2	220
Single top	14	17	8	7	5	50
QCD	623	120	60	1	6	811
Background	3251	720	338	49	37	4395
Signal	960	999	1086	331	425	3801
Total	4211	1719	1424	380	462	8196
S/B	0.3	1.4	3.2	6.8	10.6	0.9
Observed	4474	1711	1434	365	375	8359

Luminosity $\mathcal{L} = 9\ \text{fb}^{-1}$

Monte Carlo Samples

- Signal
  - PYTHIA6.2 for leading-order (LO) $\rightarrow$ Testing.
  - POWHEG for next-to-leading-order(NLO) + PYTHIA6.4 $\rightarrow$ Final Calibration.
- Background
  - ALPGEN+PYTHIA (W + *jets*) and PYTHIA (Z + *jets*).
  - MADGRAPH5 (*single top* for $m_t = 172.5$ GeV) + PYTHIA (parton shower and hadronization).
  - PYTHIA (*Diboson*).
  - Data sample (QCD background).

Matrix Element Method

- Full use of topological and kinematic information of a given event.
- Maximization of a suitable likelihood function
  - $$L_{tot} = \prod_{i=1}^{N} \left[a\left(f_{sig}\right) L_i^{sig}\left(m_t, \Delta_{JES}\right) + b\left(f_{back}\right) L_i^{back}\left(\Delta_{JES}\right) \right]$$
  - $$JES = \frac{p_T^{MC-jet}}{p_T^{Cal-jet}} = 1 + \Delta_{JES} \cdot \sigma_{p_T}^{Cal-jet}$$
- JES is constrained by the ME through the dependence of the matrix element itself on the W mass.

Matrix Element Method

Likelihood

$$L_i^{sig}\left(m_t, \Delta_{JES}\right) = \frac{1}{\sigma\left(m_t\right)} \frac{1}{A\left(m_t, \Delta_{JES}\right)} \sum_{j=1}^{24} w_{ij} \, P^{sig}\left(\vec{x}_i \middle| m_t, \Delta_{JES}\right)$$

Matrix Element Method

Likelihood

$$L_i^{sig}\left(m_t,\Delta_{JES}\right) = \frac{1}{\sigma\left(m_t\right)} \frac{1}{A\left(m_t,\Delta_{JES}\right)} \sum_{j=1}^{24} w_{ij} \, P^{sig}\left(\vec{x}_i|m_t,\Delta_{JES}\right)$$

$$P^{sig}\left(\vec{x}_i|m_t,\Delta_{JES}\right) = \int \epsilon\left(\vec{x}_i|\vec{y}_i,\Delta_{JES}\right) T\left(\vec{x}_i|\vec{y}_i,\Delta_{JES}\right) \left|M^{t\bar{t}}_{2p\to l\nu_l+4p}\left(m_t,\vec{y}_i\right)\right|^2 \times \left.\frac{f\left(z_1,Q^2\right) f\left(z_2,Q^2\right)}{z_1 z_2}\right|_{Q^2=4m_t^2} dz_1 dz_2 d\Phi\left(\vec{y}_i\right)$$

Transfer Functions

$$P^{sig}\left(\vec{x}_i|m_t,\Delta_{JES}\right)=\int\epsilon\left(\vec{x}_i|\vec{y}_i,\Delta_{JES}\right)\boxed{T\left(\vec{x}_i|\vec{y}_i,\Delta_{JES}\right)}\left|M^{t\bar{t}}_{2p\to l\nu_l+4p}\left(m_t,\vec{y}_i\right)\right|^2$$
$$\times\left.\frac{f\left(z_1,Q^2\right)f\left(z_2,Q^2\right)}{z_1z_2}\right|_{Q^2=4m_t^2}dz_1dz_2d\Phi\left(\vec{y}_i\right)$$

$$T_{old}=F_1\left(\frac{p_T^j}{p_T^p};p_T^p,\eta_p,m_p\right)\times F_2\left(\Delta\eta_{j-p},\Delta\phi_{j-p};p_T^p,\eta_p,m_p\right)$$

$$T_{new}=F_3\left(\frac{p_T^j}{p_T^p},\Delta R_{j-p};p_T^p,\eta_p,m_p\right)$$

$$\Delta R_{j-p}=\sqrt{\left(\Delta\eta_{j-p}\right)^2+\left(\Delta\phi_{j-p}\right)^2}$$

Transfer Functions

T_{old}

- Derived from PYTHIA6.2.
- Only LO.
- Angular variables factorised as $\Delta\eta_{j-p}$ vs $\Delta\phi_{j-p}$.
- T_{old} are constructed for tight event categories.

T_{new}

- Derived from POHWEG + PYTHIA6.4.
- Extra parton emission at NLO requires jet-to-parton matching.
- Angular decomposition is made through the Jacobian: $\Delta R_{j-p} \rightarrow (\Delta\eta_{j-p}, \Delta\phi_{j-p})$.
- T_{new} include also loose event categories.

Grids scanned for the T_{old} and T_{new}

- The T_{old} are projected on $\Delta\phi_{j-p}$ axis of a 2D histograms of $\Delta\eta_{j-p}$ vs $\Delta\phi_{j-p}$.
- The T_{old} are projected on $\Delta\phi_{j-p}$ axis of a 2D histograms of $\frac{p_T^j}{p_T^p}$ vs $\Delta\phi_{j-p}$.
- They both depend on m_p, p_T^p, η_p, Δ_{JES} and the parton type ($isB = 0$ for light quarks or $isB = 1$ for b-quarks).
- The kinematic variables are shown in the following table:

Central kinematics

isB	0	1	
m_p	10	20	
p_T^p	40	60	
η_p	-1	0	+1
Δ_{JES}	-2	0	+2
$\Delta\eta_{j-p}$	-0.2	0	+0.2

Wide kinematics

isB	0	1	
m_p	0.5	5	50
p_T^p	5	25	100
η_p	-2	0	+2
Δ_{JES}	-2	0	+2
$\Delta\eta_{j-p}$	-0.2	0	+0.2

Comparison of the old and new TFs

Transfer Functions

m_p	p_T	η_p	isB	Δ_{JES}
50	100	0	0	0

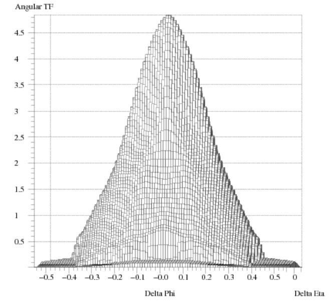

Figure: $\Delta\eta$ vs $\Delta\phi$ plot projected on $\Delta\phi$ axis for T_{old}.

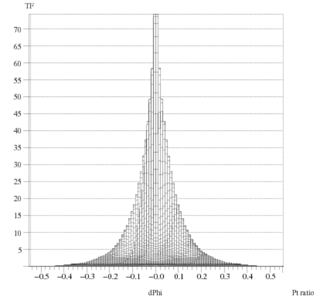

Figure: $\frac{p_T^j}{p_T^p}$ vs $\Delta\phi$ plot projected on $\Delta\phi$ axis for T_{new} with $\Delta\eta_{j-p} = 0$.

Comparison of the old and new TFs

Transfer Functions

m_p	p_T	η_p	isB	Δ_{JES}
50	100	0	1	0

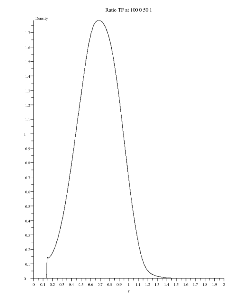

Figure: $\frac{p_T^j}{p_T^p}$ plot for T_{old}.

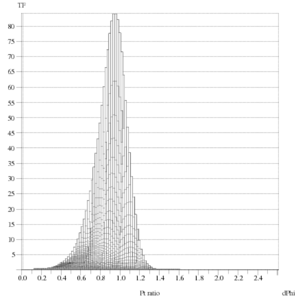

Figure: $\frac{p_T^j}{p_T^p}$ plot for T_{new} with $\Delta\eta_{j-p} = 0$.

Comparison of the old and new TFs

Transfer Functions

m_p	p_T	η_p	isB	Δ_{JES}
5	5	0	0	0

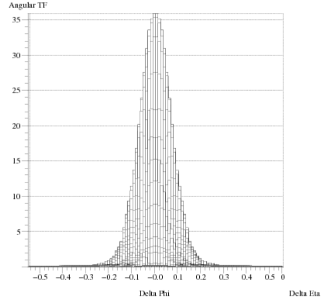

Figure: $\Delta\eta$ vs $\Delta\phi$ plot projected on $\Delta\phi$ axis for T_{old}.

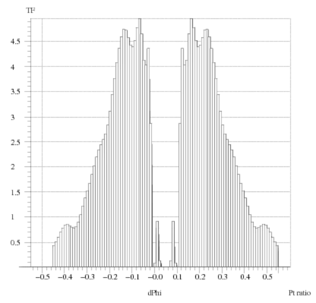

Figure: $\frac{p_T^j}{p_T^p}$ vs $\Delta\phi$ plot projected on $\Delta\phi$ axis for T_{new} with $\Delta\eta_{j-p} = 0$.

Comparison of the old and new TFs

Transfer Functions

m_p	p_T	η_p	isB	Δ_{JES}
50	5	2	0	0

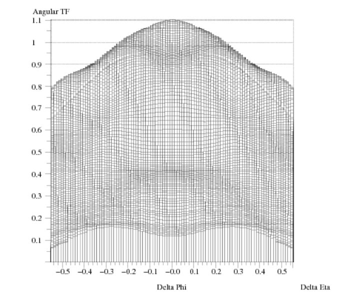

Figure: $\Delta\eta$ vs $\Delta\phi$ plot projected on $\Delta\phi$ axis for T_{old}.

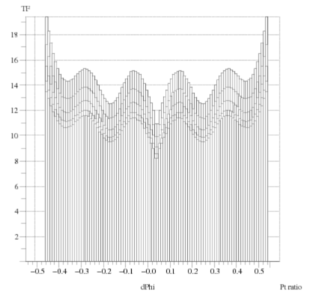

Figure: $\frac{p_T^j}{p_T^p}$ vs $\Delta\phi$ plot projected on $\Delta\phi$ axis for T_{new} with $\Delta\eta_{j-p} = 0$.

Grid scanned for the ϵ_{old} and ϵ_{new}

- The efficiencies are displayed as 2D histograms of p_T^p vs Δ_{JES}, given m_p, η_p and the parton type ($isB = 0$ for light quarks or $isB = 1$ for b-quarks).

isB	0	1				
η_p	-2	-1	0	+1	+2	
m_p	0.5	1.5	5	10	20	40

- The values $\eta_p = -2$ and $\eta_p = -1$ is chosen to show the symmetry of the efficiencies about $\eta_p = 0$.

Comparison of the old and new TFs

Efficiencies

$m_p = 0.5$ $isB = 0$ $\eta_p = \quad 0$

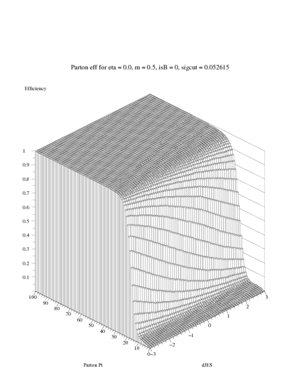

Figure: Efficiency plot for ϵ_{old}.

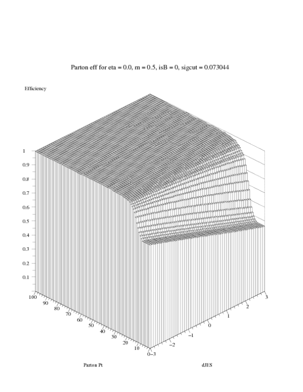

Figure: Efficiency plot for ϵ_{new}.

Comparison of the old and new TFs

Efficiencies

$m_p = 0.5$ $\quad$ $isB = 0$ $\quad$ $\eta_p = -2$

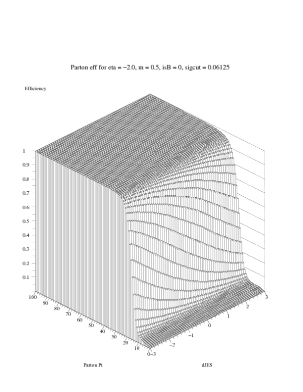

Figure: Efficiency plot for ϵ_{old}.

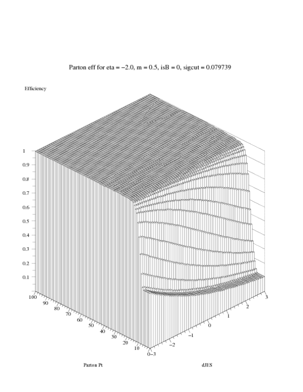

Figure: Efficiency plot for ϵ_{new}.

Comparison of the old and new TFs

Efficiencies

$m_p = 5.0$ $isB = 1$ $\eta_p = -2$

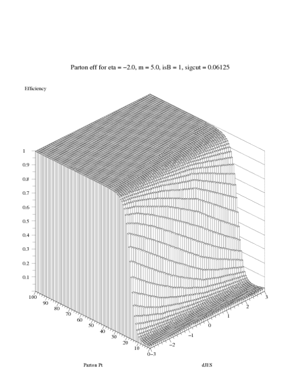

Figure: Efficiency plot for ϵ_{new}.

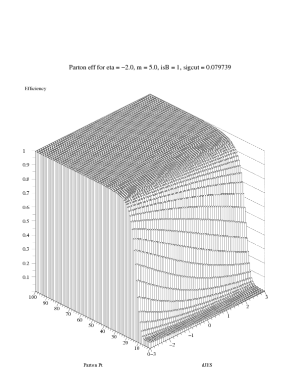

Figure: Efficiency plot for ϵ_{new}.

Comparison of the old and new TFs

Possible causes of discrepancy

- Numerical problem with decomposition for T_{new}.
- Physics differences between the MC used.
- Extra emission misidentified as a top decay product in T_{new}.

Integration method

What we do

$$\int_{[0,1]^s} f(\vec{x}) d\vec{x} \approx \frac{V\left([0,1]^s\right)}{N} \sum_{i=1}^{N} f(\vec{x}_i) \qquad \text{error } \epsilon \equiv \left| \int_{[0,1]^s} f(\vec{x}) - \frac{1}{N} \sum_{i=1}^{N} f(\vec{x}_i) \right|$$

Integration method

What we do

$$\int_{[0,1]^s} f(\vec{x})d\vec{x} \approx \frac{V\left([0,1]^s\right)}{N}\sum_{i=1}^{N} f(\vec{x}_i) \qquad \text{error } \epsilon \equiv \left| \int_{[0,1]^s} f(\vec{x}) - \frac{1}{N}\sum_{i=1}^{N} f(\vec{x}_i)\right|$$

How we do

pseudo-Monte Carlo: $\epsilon_{pMC} \propto \frac{1}{\sqrt{N}}$ quasi-Monte Carlo: $\epsilon_{qMC} \propto \frac{(lnN)^s}{N}$

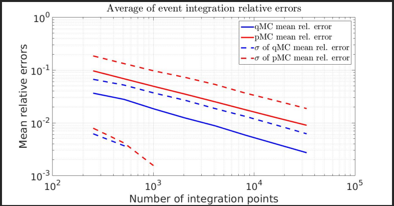

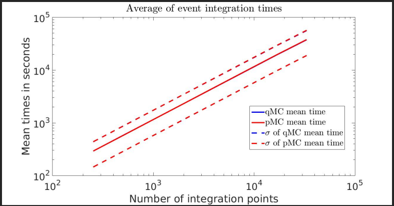

Integration method

What we do

$$\int_{[0,1]^s} f(\vec{x})d\vec{x} \approx \frac{V\left([0,1]^s\right)}{N}\sum_{i=1}^{N} f(\vec{x}_i) \qquad \text{error } \epsilon \equiv \left| \int_{[0,1]^s} f(\vec{x}) - \frac{1}{N}\sum_{i=1}^{N} f(\vec{x}_i) \right|$$

How we do

pseudo-Monte Carlo: $\boxed{\epsilon_{pMC} \propto \frac{1}{\sqrt{N}}}$

quasi-Monte Carlo: $\epsilon_{qMC} \propto \frac{(lnN)^s}{N}$

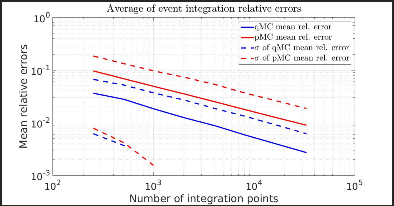

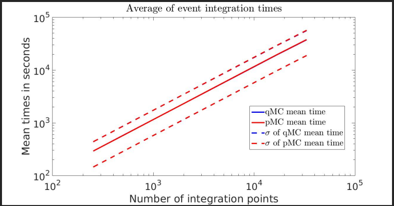

Pull Distribution

- It is the distribution of the variables

$$\delta_i = \frac{x_i - \mu}{\sigma}$$

  where μ is the arithmetic mean and σ is the standard deviation of the data x_i.

- x_i refers to the same event set but with different integration seeds.
- It has been used to analyse background event.
- It has been created through pseudo Monte Carlo samples.
- Up to now acceptance is not included.

Pull Distribution

- Pull distribution for background events (W+jets)

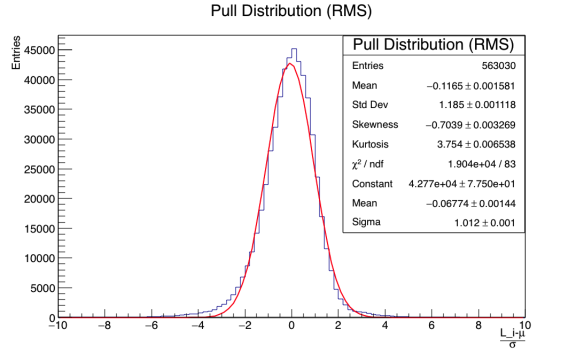

Pull Distribution

- Pull distribution for background events (W+jets)

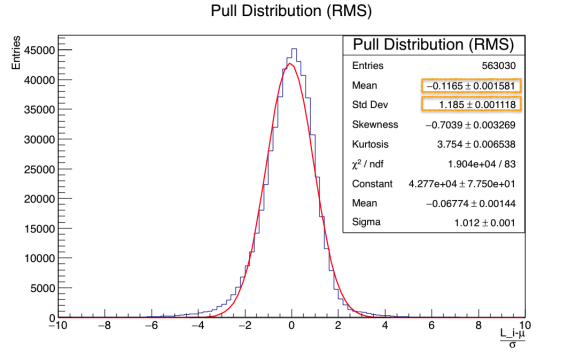

Pull Distribution

- Mean and standard deviation of pull distribution as a function of the JES shift for background events

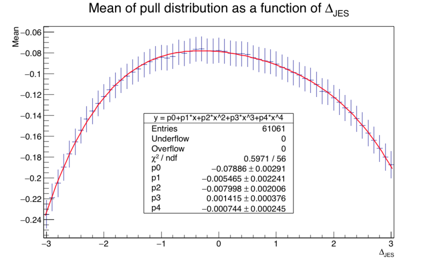

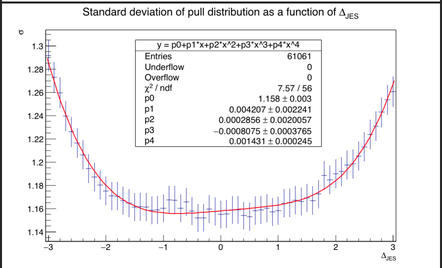

Conclusion

Summary

- Discrepancy between TFs has been noticed.
- Problem in TFs for signal events may hint problems in background TFs because of similar construction.
- Acceptance need to be included in background pulls.
- Event statistic needs to be improved for pulls.

Step to be done

- Solve differences between old and new TFs.
- Better understanding of background TFs.
- Complete background acceptance: this could lead to more precise pulls.
- Combination of signal and background likelihood.
- Lots of work yet . . .

Thanks for the attention